



# Adapting to an enhanced color gamut – implications for color vision and color deficiencies

IVANA ILIC,<sup>1</sup> KASSANDRA R. LEE,<sup>1</sup>  YOKO MIZOKAMI,<sup>2</sup>  LORNE WHITEHEAD,<sup>3</sup> AND MICHAEL A. WEBSTER<sup>1,\*</sup> 

<sup>1</sup>Department of Psychology and Graduate Program in Integrative Neuroscience, University of Nevada, Reno, USA

<sup>2</sup>Department of Imaging Sciences, Chiba University, USA

<sup>3</sup>Department of Physics and Astronomy, University of British Columbia, USA

\*mwebster@unr.edu

**Abstract:** One strategy for aiding color deficiencies is to use three narrow passbands to filter the light spectrum to increase the saturation of colors. This filtering is analogous to the narrow emission bands used in wide gamut lighting or displays. We examined how perception adapts to the greater color gamut area produced by such devices, testing color-normal observers and simulated environments. Narrowband spectra increased chromatic contrasts but also increased contrast adaptation, partially offsetting the perceived contrast enhancements. Such adaptation adjustments are important for understanding the perceptual consequences of exposure to naturally or artificially enhanced color gamut areas for both color-deficient and color-normal observers.

© 2022 Optica Publishing Group under the terms of the [Optica Open Access Publishing Agreement](#)

## 1. Introduction

Common congenital color deficiencies result from a loss (dichromacy) or alteration (anomalous trichromacy) in the spectral sensitivities of the medium- or long-wavelength sensitive (M or L) cone receptors [1]. In anomalous observers, the wavelength of peak sensitivity for the altered photopigment is shifted toward the normal pigment, reducing the normal 30-nm difference between the L and M spectral peaks to a range of 2 to 12 nm depending on the specific gene alterations [2]. The closer similarity in the L and M cone responses results in a weaker signal for the L vs M dimension of color vision conveyed by their differences.

One approach to aiding such color deficiencies is to filter the light spectrum in order to increase the differences in the L and M responses. This can be done with notch filters that block selected regions of the visual spectrum, and are the basis for commercially available filters [3–5]. The filtering can also be achieved by altering the spectrum of an illuminant or displays [6–8]. Sources with these properties are available in illumination and display devices which for example use narrowband light-emitting diodes (LEDs) to increase the gamut of available colors [9–11], and there is evidence that observers prefer moderately exaggerated colors in spite of poorer rendering [12]. For both filters and illuminants the spectral shaping works by blocking (or not emitting) wavelength bands to reduce the joint responses in the L and M cones, so that the differential responses are relatively greater. The proportional gains in the color gamut area are similar for anomalous or normal trichromats [7]. Thus, the technology has similar impact on observers with widely varying forms of color vision.

Despite the potential advantages of these techniques, the visual consequences of exposure to changes in the color gamut area are not fully understood. In this study we examined how observers might adapt to the enhanced color gamut area that spectral filtering introduces. Vision adapts over a range of timescales to most visual attributes in the observer's environment, and this adaptation has profound effects on both sensitivity and appearance [13,14]. Adaptation to

color occurs at multiple sites in the visual pathway and adjusts to distinct aspects of the stimulus [15]. Light and chromatic adaptation begin in the receptors, which adjust to the mean light levels they are exposed to [16]. However, color vision also adapts to the variation in color around the average [15]. We refer to these variations as the chromatic contrast of the color distribution, in the same way that contrast can be defined for the luminance variations in a stimulus [17]. Adaptation to chromatic contrast is a separate process from the adjustments involved in light or chromatic adaptation [15], and is thought to primarily occur at cortical levels in the visual system [18,19]. Both forms of adaptation continuously regulate sensitivity to color and have been shown to induce distinct changes to color appearance [20,21]. Moreover, both are likely to play a prominent role in calibrating color vision in natural viewing. For example, differences in the color gamuts of lush and arid scenes [22], or seasonal changes in the same environment [23,24], are sufficient to induce different states of adaptation and consequent changes in color perception. Contrast adaptation effects are also manifest in the changes that are perceived in the “colorfulness” of indoor environments under different lighting contexts [25,26]. However, while chromatic adaptation is widely recognized and routinely incorporated into models of color appearance [27], the potential impact and implications of contrast adaptation have received much less attention in applied aspects of color science.

Here, we explored the consequences of this contrast adaptation for the large contrast changes introduced by gamut-enhancing devices. Specifically, we explored how the visual system might be adapted to changes in the color distributions induced by these devices, and how this adaptation might shape how we perceive color. To test this, we adapted observers to colors shown on a monitor that simulated the chromaticities that would be generated by the same set of surfaces viewed under natural vs. narrowband illumination spectra (or filtering), and then had them match the colors across the different adaptation states. Our results suggest that even brief exposures to the higher color contrasts produced by gamut-enhancing devices leads to reductions in the sensitivity of the visual system to chromatic contrast, relative to natural spectra. While the present study was limited to testing these effects in normal trichromats, the gamut enhancements and adaptation to these enhancements are also relevant to individuals with anomalous trichromacy. Thus these effects are important for understanding the full consequences of gamut-enhancing devices on color perception for both color-normal and color-deficient observers.

## 2. Methods

### 2.1. Participants

Observers included author II and 10 additional student participants who were unaware of the specific aims of the study. Different subsets of observers were tested for different conditions, as detailed below. All observers had normal or corrected-to-normal visual acuity, and normal color vision, as assessed by the Cambridge Colour Test. Observers participated with informed consent and all procedures followed protocols approved by the University of Nevada, Reno’s Institutional Review Board.

### 2.2. Apparatus and stimuli

The stimuli were presented on an NEC MultiSync FP2141SB CRT monitor controlled by a Cambridge Research Systems ViSaGe board, which allows colors to be specified with high resolution. The monitor was calibrated using a Photo Research PR 655 spectroradiometer, with gun outputs linearized through lookup tables. The monitor was used to simulate the colors from naturalistic surfaces viewed under different illuminants in the following steps:

First, we constructed spectra for broadband and narrowband illuminants that were approximately matched in color temperature. Figure 1 shows the spectral power distributions of the two pairs of illuminants used, corresponding to a broadband (Planckian) or RGB illuminants with mean

correlated color temperatures of 4000K or 2724K. The RGB primaries roughly correspond to the three filter passbands incorporated in color-enhancing filters. However, the specific spectra were not matched to the filter spectra nor optimized to maximize the gamut enhancements.

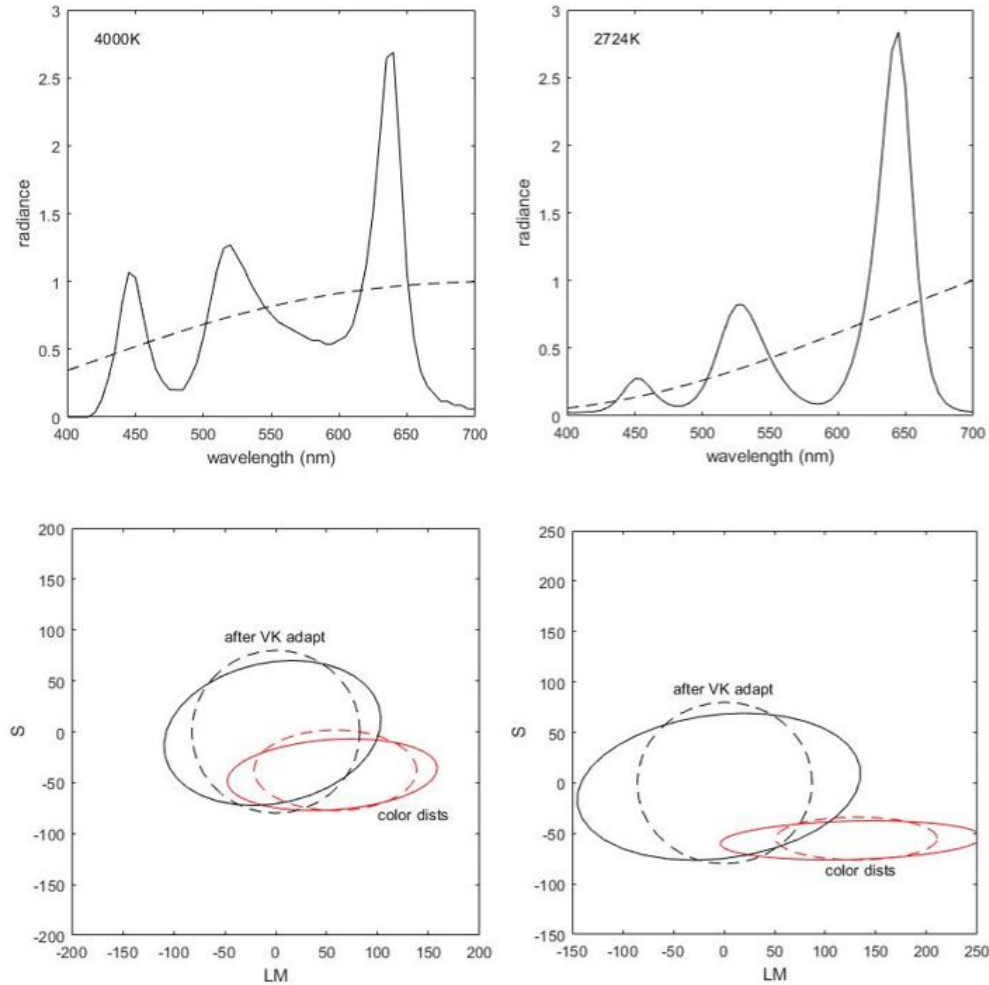


**Fig. 1.** Top. Broadband (dashed) or narrowband (solid) illuminance spectra with correlated color temperatures of 4000K (left) or 2724K (right). Bottom. Adapting color distributions for the corresponding broadband (dashed) or narrowband (solid) illuminants. The red ellipses show the coordinates of the color distributions within the LM and S chromatic plane (defined below). Note these are centered on the average chromaticity corresponding to each correlated color temperature. The black ellipses plot the chromaticities after assuming complete chromatic adaptation (von Kries adaptation) to the mean of the color distribution. In this case the distributions are centered on the origin corresponding to gray. The distributions were constructed so that for the broadband set, the colors would lie along a uniform circle centered on gray after chromatic adaptation.

Second, we simulated a set of surfaces by constructing reflectance spectra from the first three basis functions characterizing the Munsell reflectance spectra [28]. The Munsell data were selected for this purpose, because they have smoothly varying spectral patterns that are reminiscent of many natural surfaces [29]. The data available for each of these functions were interpolated to discretely sampled values at 4 nm intervals, though they of course represent

continuously varying functions of wavelength. Here, the three reflectance basis functions are denoted as  $B_i(\lambda)$ , where  $i$  is 1, 2, or 3. The corresponding reflectance spectra  $R_i(\lambda)$  are then determined by linearly combining the three basis functions, with three different weights  $c_1$ ,  $c_2$ ,  $c_3$ , as depicted in Eq. (1).

$$R_i(\lambda) = \sum_{i=1}^3 c_i B_i(\lambda) \quad (1)$$

Based on the reasonable assumption that both the simulated reflectance,  $R_i(\lambda)$ , and the illumination,  $I_i(\lambda)$ , are diffuse, then the reflected spectral radiance,  $S_i(\lambda)$ , (i.e. the light reflected by a given reflectance function  $R_i(\lambda)$  under a given illuminant  $I_i(\lambda)$ ), is simply their product. Taking into account, Eq. (1), this yields Eq. (2).

$$S_i(\lambda) = I_i(\lambda)R_i(\lambda) = I_i(\lambda) \sum_{i=1}^3 c_i R_i(\lambda) \quad (2)$$

We next defined a set of notional test surfaces, each defined by their characteristic reflectance coefficients  $c_1$ ,  $c_2$ ,  $c_3$ , so that, under the broadband illuminant, their resultant chromaticity coordinates values were uniformly distributed in a cone-opponent color space.

For this purpose, the desired chromaticity coordinates in that space are required. Those coordinates are determined by the  $l$ ,  $m$ ,  $s$  cone responses, which therefore must be calculated. As an example, the response of the L cone to a unit weight of the first Munsell basis function, under the broadband illuminant  $I_b(\lambda)$  would be given by:

$$W_{L1b} = \int L(\lambda)I_b(\lambda)B_1(\lambda)d\lambda \quad (3)$$

Considering the nine permutations yields a 3X3 matrix,  $\mathbf{W}$ , that converts the reflectance coefficients  $c_1$ ,  $c_2$ ,  $c_3$  under the broadband illuminant, to the resultant  $l$ ,  $m$ ,  $s$  cone excitations, as depicted in Eq. (4).

$$\begin{bmatrix} l \\ m \\ s \end{bmatrix} = \begin{bmatrix} W_{L1b} & W_{L2b} & W_{L3b} \\ W_{M1b} & W_{M2b} & W_{M3b} \\ W_{S1b} & W_{S2b} & W_{S3b} \end{bmatrix} \begin{bmatrix} c_1 \\ c_2 \\ c_3 \end{bmatrix} \quad (4)$$

Equation (4) is depicted more concisely in Eq. (5), where  $\mathbf{p}$  is the ordered triple of cone responses arising from  $\mathbf{c}$ , the ordered triple of reflectance coefficients.

$$\mathbf{p}_b = \mathbf{W}_b \mathbf{c}_b \quad (5)$$

Left-multiplying both sides of Eq. (4) by the inverse matrix,  $\mathbf{W}_b^{-1}$ , yields the needed result in Eq. (6).

$$\mathbf{c}_b = \mathbf{W}_b^{-1} \mathbf{p}_b \quad (6)$$

The cone stimulation values were then displayed on the monitor, by converting to the corresponding RGB values for the display.

The final step was to switch from simulating the situation under the broadband illuminant to that expected with a narrowband illuminant. In this case, the  $c_1$ ,  $c_2$ ,  $c_3$  values obtained using the broadband illuminant are retained, but this time, in Eq. (3), the broadband spectral power distribution,  $I_b(\lambda)$ , is replaced by the second narrowband illuminant characterized by spectral power distribution  $I_n(\lambda)$ . That is, Eq. (5) is changed into Eq. (7).

$$\mathbf{p}_n = \mathbf{W}_n \mathbf{c}_b \quad (7)$$

Thus,  $\mathbf{W}_n$  is determined as in Eq. (4), except using  $I_n(\lambda)$  instead of  $I_b(\lambda)$  in determining the values obtained from Eq. (3). In this way, it was possible to (1) create an accurate display-based simulation of a set of reasonable natural surface samples, illuminated by a broadband illuminant,

and having a uniform distribution of chromaticity coordinates, and (2) to model the resultant changes of those chromaticity coordinates that would arise from switching from the broadband illuminant to a specified narrowband illuminant.

The cone values for the stimulus set were selected based on chromaticities defined within the LvsM and SvsLM cone-opponent space of MacLeod-Boynton [30] and Derrington, Krauskopf and Lennie [18], which represent color in terms of the relative cone-opponent responses for a standard 2-deg observer. Within these spaces the chromatic plane at constant luminance is defined by two axes corresponding to L vs. M cone excitation (the  $r$  coordinate in the original MacLeod Boynton diagram) or variations in S cone vs. L and M cone excitation (the  $b$  coordinate in the MacLeod-Boynton space). Our version of the space was related to the MacLeod-Boynton  $r, b$  coordinates by the following equations:

$$\begin{aligned} LvsM &= (r - 0.6568) * 1955 \\ SvsLM &= (b - 0.01825) * 5533 \end{aligned} \quad (8)$$

where the nominal gray point was set at the chromaticity of Illuminant C and the scaling factors roughly equated the magnitude of perceived differences along the two axes [31]. The mean luminance of the stimuli and the background was 20 cd/m<sup>2</sup>.

The stimuli were chosen to define a uniform circle of chromaticities in the LvsM and SvsLM plane, assuming the broadband illuminant and complete chromatic adaptation to the mean chromaticity of the illuminant (modeled as independent gain changes in the cones so that after adaptation the mean had the chromaticity of the nominal gray [21]). We then simulated the distribution of color signals for the same set of surfaces under the narrowband illuminant. The set of stimuli defining the adapting distributions is shown in the bottom panels of Fig. 1.

For these distributions, the chromatic “contrast” of an individual surface corresponds to the difference from the neutral chromaticity. For example, the set of colors illustrated by the black dashed line in Fig. 1 all have a contrast of 80 because they lie along a circle centered on the gray point and with a radius of 80 in our cone-opponent space. Note that the LvsM contrasts for the same surfaces are increased under the narrowband illuminant (solid black lines in Fig. 1), illustrating the contrast enhancements under the narrowband illuminant. For the distributions as a whole, the contrast can be specified by standard metrics such as rms contrast (the standard deviation of the individual contrasts), though the effects we examine are not dependent on the choice of metrics, but only on the fact that the variations in LvsM contrast are amplified under the narrowband illuminant relative to the broadband illuminant.

### 2.3. Procedure

In three experiments, we examined the consequences of adaptation to the difference in LvsM contrast for the broadband vs. narrowband illuminants. The different experiments differed in whether the colors observers adapted to and matched were presented as uniform fields (experiments 1 and 2) or spatial patterns (experiment 3), and whether they adapted to only a single gamut (experiments 1 and 3) or simultaneously to different gamuts presented in different visual locations (experiments 2 and 3). For all conditions, the observers viewed the display binocularly at a distance of 150 cm, in an otherwise dark room, and used a keypad to record their responses. The adapting, test, and match stimuli were always shown in fields separated by a central fixation cross, and observers were instructed to maintain fixation on the cross throughout the experiment.

#### 2.3.1. Experiment 1: adaptation to an individual gamut

The first experiment examined the absolute magnitude of chromatic and contrast adaptation to the color gamut area for each illuminant, by using an asymmetric matching task to compare color appearance between fields under adaptation to the illuminant vs. a zero-contrast gray [21]. The stimuli were shown in two 4-deg fields above and below fixation (Fig. 2). Observers adapted

for 3 minutes to a random sequence of the chromaticity for either the broadband or narrowband illuminant in the top field. In this case measurements were only conducted for the 4000k set. The adapt distribution formed a set of 16 chromaticity values centered on the illuminant mean, and were chosen to have a fixed contrast of 80 after assuming complete adaptation to the mean chromaticity (Fig. 1). During adaptation observers viewed a random sequence of stimuli from the distribution, with a new color sampled every 200 ms. This simulates the pattern of temporal variation that might result from random successive eye movements sampling a scene composed of these chromaticities. A test stimulus with a fixed chromaticity was then presented for 500 ms in the adapt field, and observers matched the appearance of the test stimulus by using a keypad to adjust the hue angle (direction within the chromatic plane) and contrast (distance from the gray point) of a comparison stimulus shown at the same time as the test, but within the gray adapting field. The test stimulus was shown repeatedly and interleaved with 4-sec readaptation to the adapting stimuli in order to maintain the adaptation, with the cycle repeated until the observer completed the match, after which the program presented the next test stimulus. The test stimuli consisted of 16 hues at steps of 22.5 deg, and a contrast of 40 relative to the mean of the illuminant. Note that the test stimuli had the same chromaticity for the broadband and narrowband adapting conditions after assuming complete chromatic adaptation (i.e., they were not the chromaticity values of the simulated surfaces). This was to allow us to use identical tests to probe differential adaptation under the two illuminants. To isolate the effects of chromatic and contrast adaptation, matches were also made after adapting to the uniform mean chromaticity of the gamuts rather than to the individual samples from each gamut. In this case the adapting field showed the mean chromaticity of the gamut throughout. Because the means were very similar, this was tested for only a single mean level for two of the three observers. For each adapting condition, the observer made matches to each test 4 times in counterbalanced order. Results reported are based on the means of the matches and are statistically analyzed both at the group level and for the repeated matches made by each individual observer.

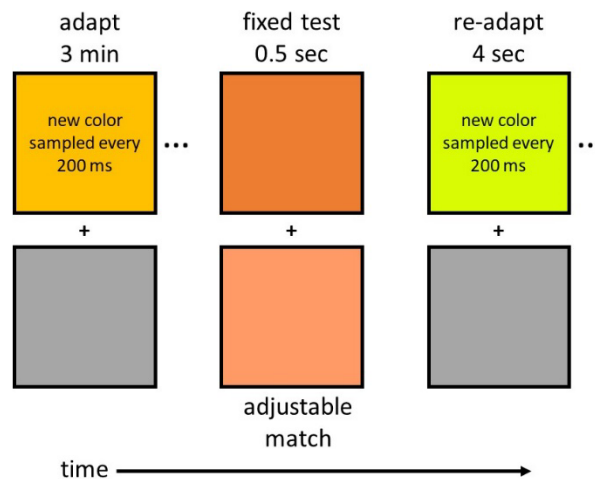


**Fig. 2.** Schematic of the procedure for adapting to a single gamut. Observers fixated the cross while the gamut colors were shown in the field above fixation for 3 min (with a new color resampled from the gamut every 200 ms). A test with a fixed chromaticity was then shown in the adapt field for 500 ms. Observers adjusted the chromaticity of the lower field to match the perceived color of the test, while the test presentations were alternated with 4-sec periods of readaptation to the color gamut. Colors are for illustrative purposes only.

### 2.3.2. Experiment 2: simultaneous adaptation to the broadband or narrowband gamuts

To gain a more sensitive comparison of the *relative* adaptation induced by the broadband and wide gamut area conditions, in the second experiment observers simultaneously adapted for 3 minutes to a random sequence of the same set of surfaces under both the broadband and narrowband conditions, but shown in the top and bottom field, respectively (Fig. 3). In this case the adaptation effects were tested only for the 2724K gamuts. The adapt and test stimuli and sequence were otherwise similar to the preceding experiment. However, in this case the two adapting gamut areas were shown at the same time within the different fields. Specifically, during the adaptation, the same random sequence of surfaces was shown in both fields but under the two different illuminants. During testing, observers matched the appearance across the two fields by adjusting the relative hue and contrast of a test stimulus now also shown in both fields. The test pair were yoked so that increasing the hue angle or test contrast in the top field reduced the value in the bottom field, or vice-versa. Once again each observer made 4 matches to each of the 16 test stimuli, with the order counterbalanced across trials.

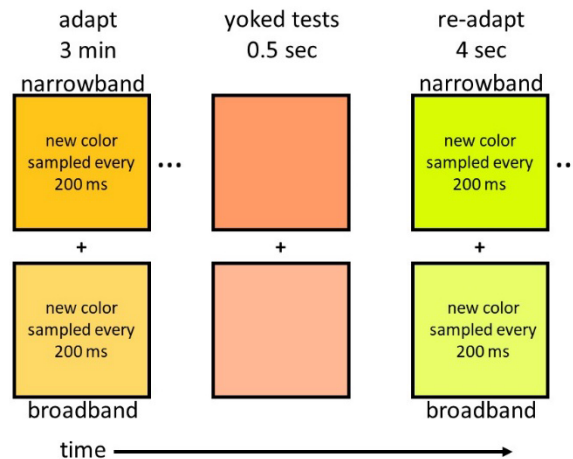


**Fig. 3.** Schematic of the procedure for simultaneously adapting to the broadband and narrowband gamuts. Observers fixated the cross while the gamut colors for one illuminant was shown in the upper field and for the other illuminant in the lower field. During the initial for 3 min adaptation corresponding colors from the two gamuts were resampled every 200 ms. A pair of test stimuli were then shown in the two fields for 500 ms. Observers adjusted their relative contrast and hue angle until they appeared to match. The adjustments were made while the test presentations were alternated with 4-sec periods of readaptation to the two color gamuts. Colors are for illustrative purposes only.

### 2.3.3. Experiment 3: adaptation to the color gamuts in spatial patterns

The final experiment was designed to generalize the preceding conditions to more naturalistic viewing conditions, by adapting to spatially varying color distributions – or images. In this case the stimuli were shown in two 7-deg x 5.5-deg fields, now on the left and right of the fixation cross, and were filled with patterns composed of random overlapping rectangles, commonly described as “Mondrian” patterns [32] (Fig. 4). The left and right images had the same spatial pattern but were mirrored to aid comparing them. The color coordinates of the rectangles were drawn from the 2724K color distributions for the two illuminants, but after first adjusting for a gray mean in order to emphasize the contrast differences between the distributions (i.e. the color distributions corresponded to the color signals after complete chromatic adaptation in Fig. 1).

The colors were also now varied randomly in luminance so that the images had an rms luminance contrast of 0.2. As before, observers adapted to random sequences of the colors shown in the Mondrians every 200 ms. Following adaptation a pair of test Mondrians was displayed for 500 ms. The chromatic contrast of the test stimuli was on average the same as the broadband condition (i.e. hue angles forming a circle with a nominal contrast of 80). The S vs. LM contrast remained fixed at this value, and observers varied the L vs. M contrast above or below 80 to match the perceived contrast across the two adapting fields. As in Experiment 2, the test pair were yoked so that increasing the test contrast in the right field reduced it in the left field, or vice-versa.

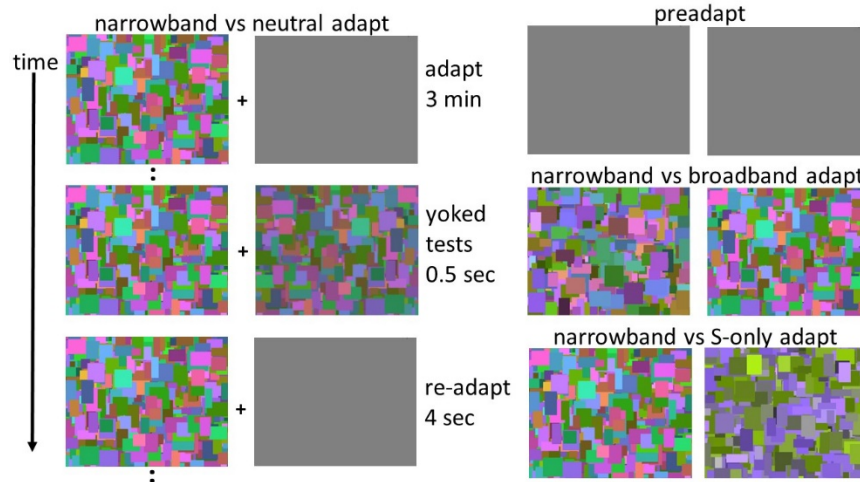


**Fig. 4.** Left side: schematic of the procedure for simultaneously adapting to the narrowband vs. neutral gray presented as Mondrian patterns. Observers fixated the cross while the Mondrian was shown on one side and a gray field on the other. During the initial 3-min adaptation period Mondrians with the same gamut were resampled every 200 ms. A pair of test Mondrians were then shown in the two fields for 500 ms. Observers adjusted their relative LvsM contrast until they appeared to match. The adjustments were made while the test presentations were alternated with 4-sec periods of readaptation to the color gamut. Right side: illustration of the 3 other adapting conditions tested (see text). Colors are for illustrative purposes only.

To fully assess the contrast changes, we measured the matches for 4 conditions, which varied in the degree to which the colors varied between the two adapting fields. The corresponding images are illustrated in Fig. 4.

- 1) Pre-adapt: adaptation was to the same static gray field on both sides. Thus, the matches for the test Mondrians should occur when the two sides had the same physical contrasts. This case thus assessed the ability to correctly set the matches.
- 2) Narrowband vs. broadband gamut: observers adapted to the set of Mondrians simulated under the broadband illuminant on one side and the narrowband illuminant on the other side, to assess the relative differences in adaptation to the two distributions. This condition paralleled the adapted contrasts shown as temporal variations in Experiment 2.
- 3) Narrowband vs. S-only contrast: In this condition one adapting field displayed the enhanced gamut distribution while in the other the LvsM contrast was set to zero so that the Mondrian only varied in SvsLM and luminance contrast. This was tested to isolate the contribution of the overall LvsM contrast to the changes in perceived contrast.

- 4) Narrowband vs. neutral: this condition compared adaptation between the enhanced color gamut and a neutral gray field to examine the absolute magnitude of the contrast adaptation.

On each run observers adapted to one of the 4 adapting conditions, and then made 10 repeated matches of the L vs. M contrasts. Results reported are based on 2 runs or 20 matches for each condition, with the order of the adapting conditions counterbalanced.

### 3. Results

#### 3.1. Predicted adaptation effects

Figure 5 illustrates the predicted changes in the appearance of the test stimuli following adaptation to the mean and contrast of the color distributions. The ellipses on the lower right represent the pre-adapt LvsM and SvsLM coordinates for the surfaces under the broadband or narrowband illuminants. Again, these were chosen to have an equivalent mean chromaticity which (under neutral adaptation) is yellow and thus plots in the lower right quadrant of the space. The circle and ellipse in the upper left represent the predicted coordinates after complete chromatic adaptation to the illuminant, so that the stimuli are now centered on the gray point. The shift in appearance due to adaptation to the mean color is signified by the blue arrow, and should be common for the broadband and narrowband conditions because they were chosen to have a common mean. (Note the expansion of the signals along the SvsLM axis is because of the multiplicative rescaling of the cone signals with chromatic adaptation. The same rescaling within the L and M cones has opposing effects along the LvsM axis so that the signal differences remain more similar along this axis). The chromaticity values under the narrowband condition are stretched along the LvsM axis, forming more elliptical contours. However, the higher LvsM contrasts in this case should result in stronger contrast adaptation, reducing perceived contrast more for this adapting stimulus. These contrast losses are indicated by the red arrows. If adaptation completely normalizes the contrast response, this predicts that the colors of the different adapting distributions should appear the same when the observer is fully adapted to either condition.

#### 3.2. Experiment 1: adaptation to the individual broadband or narrowband conditions

As noted, in the first case we empirically assessed the adaptation for the individual gamuts by comparing color appearance after adapting to the broadband or narrowband gamut conditions vs. a uniform gray field. Figure 6 plots individual measurements for the three observers tested. In this case, the two illuminants tested had a color temperature of 4000K. The lower-right points represent the test stimuli (before adaptation). The filled and unfilled red points represent the matches for these stimuli after adaptation to the broadband or narrowband gamut conditions, respectively. Finally, the upper-left black points represents the settings for adaptation to only the mean chromaticity. For all subjects, the matches show strong, but incomplete chromatic adaptation. That is, the matching coordinates are strongly shifted toward the neutral gray but have a residual yellowish bias in the mean. Both the broadband and narrowband distributions also produced pronounced contrast adaptation. Specifically, the match contrasts for the adapting sequence are substantially lower than when adapted to the static illuminant mean. However, in this case the magnitude of contrast adaptation appears similar for the two illuminants. To assess this, we compared the magnitude of the LvsM matching contrasts relative to the sample mean for each observer. For all 3 observers, t-tests indicated that there was not a statistically significant difference in magnitude of matching contrasts for the natural vs. wide gamut condition [ $t(30) = .58, p = 0.56$ ;  $t(30) = 1.21, p = 0.23$ ;  $t(30) = .31, p = 0.75$ , for the 3 observers]. Thus, while this experiment confirmed the strong chromatic and contrast adaptation effects for both conditions, it did not reveal clear differences in adaptation between the broadband or narrowband conditions.

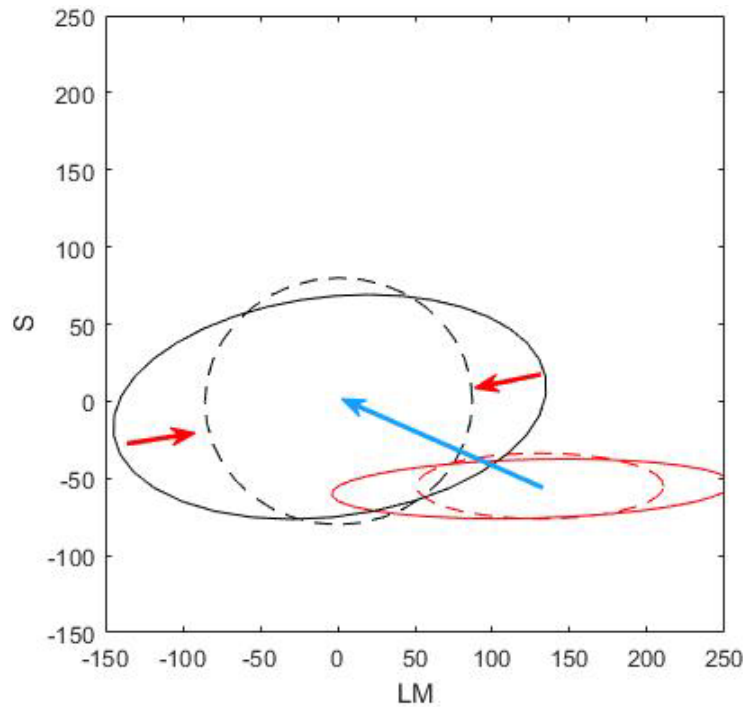


**Fig. 5.** Predicted chromatic shifts with adaptation. Red ellipses show the color coordinates of the broadband (dashed) and narrowband (solid) adapting distributions under neutral adaptation. Chromatic adaptation to the mean of the adapting distributions recenters the perceived mean color to appear gray (blue arrow). Contrast adaptation to the variance in the adapting distributions reduces the perceived contrasts or gamut of the distributions (red arrows). This contrast adaptation should be stronger for the narrowband condition since it generates higher stimulus contrasts.

### 3.3. Experiment 2: simultaneous adaptation to broadband vs. narrowband gamut conditions

To provide a more sensitive measure of differential adaptation to the broadband or narrowband conditions, we turned to the second experiment where both gamuts were displayed simultaneously in the two fields, and then measured the differences in color appearance between the two fields. Unlike the preceding measurements, this condition cannot reveal the absolute changes in chromatic or contrast adaptation common to both gamuts, but provides a more direct measure of any differences in the adaptation effects between them.

Figure 7 show the matches between adaptation to either condition (this time tested for the color temperature of 2724K) for each of the 6 observers tested, along with the average across observers. The black triangles represent the matching values in the field adapted to the broadband gamut and the red lines and circles represent the matches for the narrowband gamut. In this case, the matches required consistently higher contrast along the LvsM axis for the field adapted to the enhanced gamut condition. Specifically, the matching contrasts along the LvsM axis were on average 1.17 times higher for the narrowband illuminant condition than for the broadband illuminant. These differences were assessed with paired t-tests of the LvsM contrast for the 16 test stimuli and were significant for each of the six observers ( $t(15) \geq -3.61$ ,  $p \leq .002$  for all observers). The contrast differences are consistent with a sensitivity loss induced by stronger adaptation to the stronger red-green contrast created by the filtered spectrum.

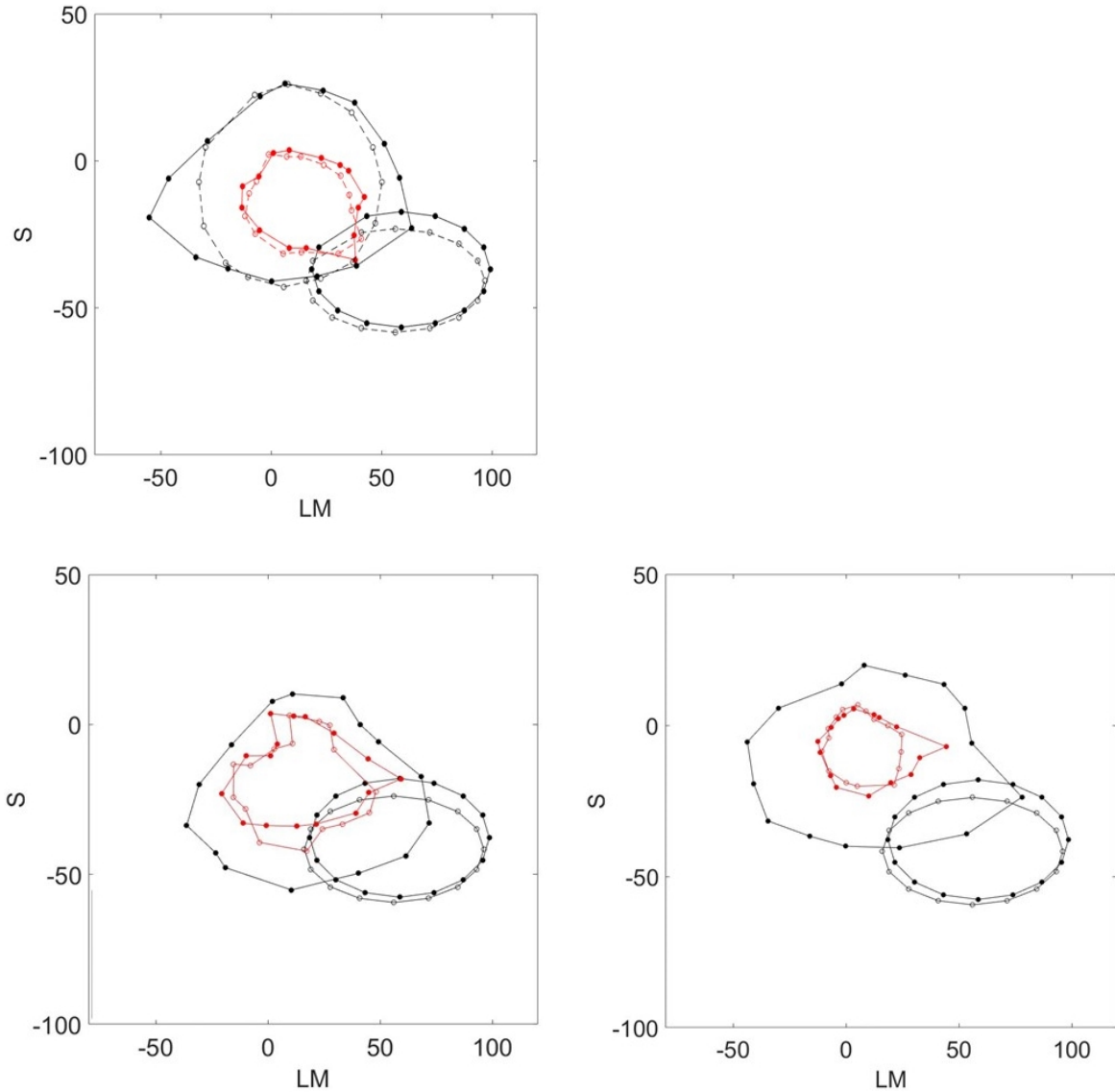


**Fig. 6.** Changes in color appearance following adaptation to the 4000 K broadband or narrowband gamuts for 3 observers. Black symbols and lines at the lower right show the chromaticities of the test colors presented in the adapting field. Red symbols show the coordinates of the matching chromaticities for the narrowband (open symbols) or broadband adapting gamuts (filled symbols). Black symbols at the upper left instead show the matches after adaptation to the static mean chromaticity (tested for only one gamut mean for two of the observers).

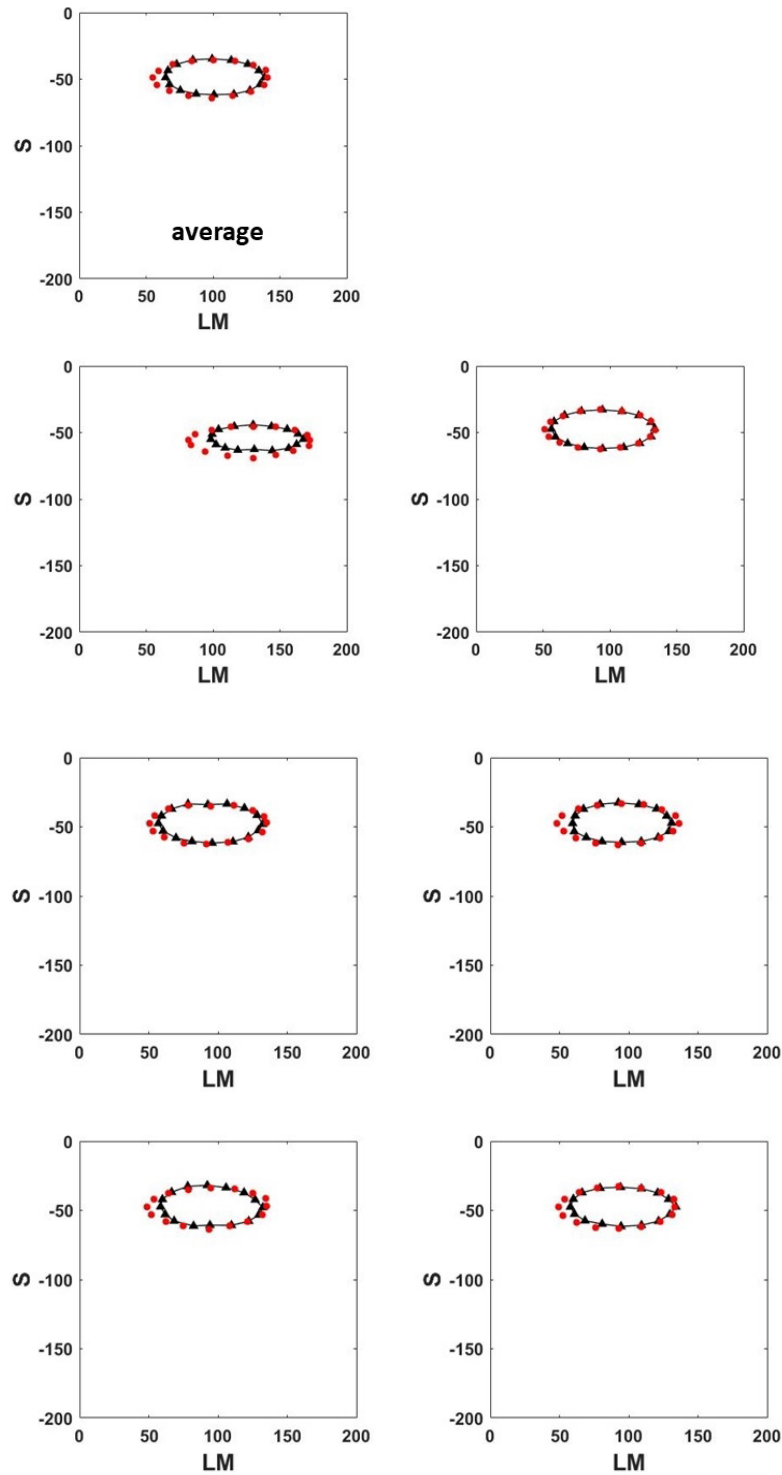


**Fig. 7.** Contrast matches made between fields adapted to the broadband or narrowband gamut conditions for the 2724 K illuminants. Red circles plot the matching contrasts in the narrowband adapt field while black triangles and lines shows the match coordinates in the broadband gamut adapt field.

### 3.4. Experiment 3: adaptation to color contrast in spatial patterns

The final set of experiments were again designed to confirm the differential adaptation effects for the different color gamut areas, but for spatially varying stimuli that presented the adapting

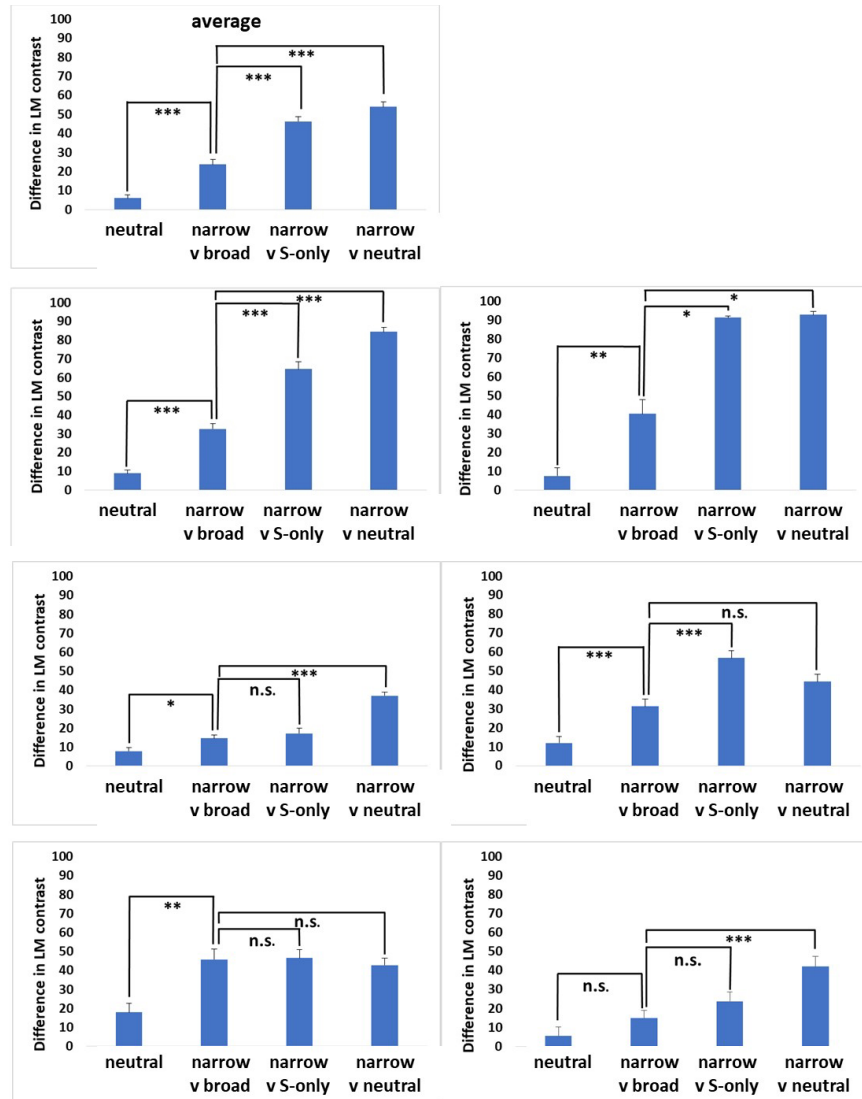


**Fig. 8.** Contrast matches between the two Mondrian fields after adapting to different levels of LvsM contrast. Bars plot the difference in percent change in LvsM contrast between the two fields +1 SEM. A value of zero represents a physical contrast match. Neutral: matches under neutral (uniform gray field) adaptation in both fields. narrow vs broad: difference between the match values in the narrowband vs. broadband gamut conditions. Narrow vs. S-only: matches for the narrowband adapt gamut minus the settings for the same gamut with the LvsM contrasts removed. Narrowband vs. neutral: differences in the matching contrasts following adaptation to the narrowband vs. gray adapt conditions. Individual plots show matches for the six individual observers and averaged across the observers. \*  $p < 0.017$  (corrected for multiple comparisons); \*\*  $p < 0.001$ ; \*\*\*  $p < .0001$ ).

gamut areas in Mondrian displays rather than uniform fields. The task in this case was to match the LvsM contrast in the Mondrians after adapting to the narrowband gamut areas vs. the control gamut areas. These effects were again tested only for the 2724K condition and after adjusting for chromatic adaptation to the neutral gray chromaticity. Figure 8 shows the contrast ratio between the two adapting fields for each condition for each of the six observers tested, along with the mean across observers. Bars indicate the mean difference in percent change between the matched LvsM contrasts + 1 SEM. As expected, the pre-adapt conditions are close to a physical match. However, for the remaining conditions adaptation to the field with higher LvsM contrast reduced the perceived contrast in the Mondrians relative to the second adapting field, and thus the contrast had to be increased in the high-contrast field to make the match. There was a significant difference between conditions for each observer as determined by a one-way ANOVA ( $F(3,72) \leq 8.25, p < .0001$  for all observers). Post hoc comparisons (Bonferroni corrected within each observer) revealed that matches required more LvsM contrast in the narrowband vs. broadband condition for 5 of 6 observers and for the overall mean (see Fig. 6). As expected, the differences for these conditions also tended to be smaller than for the narrowband vs. S-contrast only or gray-field conditions – for which the LvsM adapting differences were much larger. However, for some observers the magnitudes of these effects were similar to the narrowband vs. broadband gamut areas. Thus the results again reveal substantial differential contrast adaptation, consistent with the results for Experiment 2, and again suggest that exposure to the higher color gamut area caused that gamut to appear reduced in contrast compared to the broadband gamut condition.

#### 4. Discussion

In this study, we systematically investigated how the visual system might adapt to short-term changes in the color environment induced by increasingly common devices designed to increase the chroma of colors. Consistent with previous studies our results show that states of chromatic adaptation remain similar after exposure to natural or filtered color signals that have the same mean chromaticity but produce different gamut areas [20,21]. However, side-by-side comparisons (experiments 2 and 4) reveal significant differences in the amount of contrast adaptation that the differences in spectral filtering produce. Specifically, the wider gamut area generated by the filtered lighting led to significantly greater contrast adaptation. The changes in perceived contrast are largely specific to the LvsM axis along which the gamut areas differed, consistent with the color-selectivity that has been observed previously in color contrast adaptation [31,33]. While the pattern of adaptation effects we measured are thus predictable, what is important and shown here is that they can be manifest for the changes in color gamuts introduced by methods designed to enhance color signals for observers. Our results are also important for highlighting the importance of contrast adaptation as a significant factor in assessing the perceptual consequences of filtering or lighting conditions that alter the range of color contrasts observers are exposed to.

Again, these filtering and emissive devices have been developed for enhancing color percepts for both color-normal and color-deficient observers. In our study we assessed the adaptation effects only on normal trichromats, and thus it will be important to extend these measurements to explore their magnitude and form in anomalous trichromats. However, there is good reason to think that the consequences will be similar. Typical congenital changes in color vision affect only the photopigments and thus leave the neural machinery for color vision largely intact [1]. Adaptation is a ubiquitous and intrinsic feature of sensory coding, and there is no reason to expect that the mechanisms of adaptation themselves would be different in color deficient observers. In fact, several studies have suggested that because of processes like adaptation, the sensitivity losses in anomalous trichromats may be partially compensated by post-receptoral amplification of the weakened LvsM chromatic signals provided by their cones [2,34]. That is, the color losses in these observers may be less severe than their cone sensitivities predict, because neural gain has been adjusted to the weakened gamut of their cone signals. A number of behavioral

tasks have been used to reveal better-than-expected color percepts in anomalous trichromats [35–40], and a recent fMRI study found evidence for the amplification of LvsM color signals in early visual cortex in anomalous trichromats, consistent with the cortical locus of color contrast adaptation [41]. Further evidence for compensatory cortical gain has come from measures of visual evoked potentials (though this has been reported for binocular but not monocular viewing) [42]. Thus, both the neural responses to chromatic stimuli and the adaptation states of anomalous trichromats may already be partially compensated and thus more similar to normal trichromats than the differences in their cone spectral sensitivities predict, again consistent with an adaptive normalization of contrast coding in the visual system.

How these adaptive adjustments impact color perception for gamut-enhancing devices will also depend on the dynamics of the adaptation. For short-term exposures, contrast adaptation effects tend to build up exponentially during adaptation, and similarly can decay exponentially after the adapting stimulus is removed [43,44]. However, some color aftereffects can last a very long time pointing to multiple timescales for the adaptation [45]. Similar evidence for multiple timescales and dynamics have also been found for contrast adaptation [46]. Moreover, the dynamics of adaptation can itself change with repeated exposures [47,48]. The variety of these effects leave open the possibility that routine exposure to the contrast changes produced by gamut-enhancing devices could introduce both short and long-term changes in color appearance.

It will also be important to explore the magnitude of these adaptation effects under more natural viewing conditions. Our studies used highly controlled stimulus exposures that clearly differ from the patterns of exposure and sampling that would result with natural scenes. However, selective color contrast adaptation effects are pronounced for natural color gamut areas [22], and adaptation can be routinely observed for many aspects of natural images [13].

An important property of adaptation is that it tends to normalize visual coding [13]. In the case of color this includes shifting appearance so that the average color appears more neutral (gray) and the range of contrasts along different color and luminance axes appear more balanced [15,49]. This predicts that adaptation to enhanced gamut areas should tend to desaturate the colors under that condition so that they start to appear more natural. In turn this could lead actual natural gamut areas to appear unnatural or reduced in contrast. However, adaptation is certainly not the only form of visual plasticity, and some perceptual adjustments may elevate rather than habituate the responses to color after exposure to an enhanced color gamut. For example, Werner et al. [4] tested color percepts in anomalous trichromats after wearing color-enhancing filters. After a few days experiencing the glasses, the salience of colors increased, even with the glasses removed. Such effects may reflect a form of perceptual learning and how color was interpreted or attended to. Further characterization of these different forms of plasticity and the extent to which they occur in real environments will be important for assessing the consequences of changes in the individual's chromatic diet.

## 5. Conclusions

Modern technology has led to a number of devices for shaping the light spectrum in ways that increase the color gamut, and these are seeing potential use for both color-normal and color-deficient observers. We have shown that known processes of adaptation may partially counteract these enhancements, by renormalizing perception for the changes in the color environment. This renormalization has important implications for understanding how both color-normal and color-anomalous observers will experience color as seen in gamut-enhanced displays and lighting or color-enhancing filters. In turn, that understanding has the potential to inform the design of spectral power distributions that better suit the needs of color-normal observers as well as those who experience some kinds of color vision deficiencies.

**Funding.** National Eye Institute (EY-010834).

**Disclosures.** None to declare.

**Data availability.** Data underlying the results presented in this paper are not publicly available at this time but may be obtained from the authors upon reasonable request.

## References

1. J. Neitz and M. Neitz, "The genetics of normal and defective color vision," *Vision Res.* **51**(7), 633–651 (2011).
2. J. Bosten, "The known unknowns of anomalous trichromacy," *Curr. Opinion in Behavioral Sci.* **30**, 228–237 (2019).
3. L. Gomez-Robledo, E. M. Valero, R. Huertas, M. A. Martinez-Domingo, and J. Hernandez-Andres, "Do EnChroma glasses improve color vision for colorblind subjects?" *Opt. Express* **26**(22), 28693–28703 (2018).
4. J. S. Werner, B. Marsh-Armstrong, and K. Knoblauch, "Adaptive Changes in Color Vision from Long-Term Filter Usage in Anomalous but Not Normal Trichromacy," *Curr. Biol.* **30**(15), 3011–3015.e4 (2020).
5. J. Rabin, F. Silva, N. Trevino, H. Gillentine, L. Li, L. Inclan, G. Anderson, E. Lee, and H. Vo, "Performance enhancement in color deficiency with color-correcting lenses," *Eye (Lond)* (2022).
6. S. Tamura, Y. Okamoto, S. Nakagawa, T. Sakamoto, and Y. Shigeri, "Practical color barrier-free illumination for deuteranopia using LEDs," *Color Res. Appl.* **40**(3), 218–223 (2015).
7. D. S. Joyce, L. A. Whitehead, and M. A. Webster, "Wide gamut lighting and color contrast in anomalous trichromacy," *Proc. SPIE* **11814**, 118140D (2021).
8. S. Tamura, Y. Okamoto, S. Nakagawa, T. Sakamoto, M. Ando, and Y. Shigeri, "Light wavelengths of LEDs to improve the color discrimination in Ishihara test and Farnsworth Panel D15 test for deuterans," *Color Res. Appl.* **42**(4), 424–430 (2017).
9. X. Feng, W. Xu, Q. Han, and S. Zhang, "LED light with enhanced color saturation and improved white light perception," *Opt. Express* **24**(1), 573–585 (2016).
10. H. J. Kim, M. H. Shin, J. Y. Lee, J. H. Kim, and Y. J. Kim, "Realization of 95% of the Rec. 2020 color gamut in a highly efficient LCD using a patterned quantum dot film," *Opt. Express* **25**(10), 10724–10734 (2017).
11. M. Tsuchida, K. Hiramatsu, and K. Kashino, "Designing Spectral Power Distribution of Illumination with Color Chart to Enhance Color Saturation," in *roc. IS&T 24th Color and Imaging Conference (CIC24)* (2016), pp. 278–282.
12. M. Wei and K. W. Houser, "Systematic changes in gamut size affect color preference," *Leukos* **13**(1), 23–32 (2017).
13. M. A. Webster, "Visual adaptation," *Annu. Rev. Vis. Sci.* **1**(1), 547–567 (2015).
14. C. W. Clifford, M. A. Webster, G. B. Stanley, A. A. Stocker, A. Kohn, T. O. Sharpee, and O. Schwartz, "Visual adaptation: neural, psychological and computational aspects," *Vision Res.* **47**(25), 3125–3131 (2007).
15. M. A. Webster, "Human colour perception and its adaptation," *Network: Comput. in Neural Systems* **7**(4), 587–634 (1996).
16. F. Rieke and M. E. Rudd, "The challenges natural images pose for visual adaptation," *Neuron* **64**(5), 605–616 (2009).
17. E. Peli, "Contrast in complex images," *J. Opt. Soc. Am. A* **7**(10), 2032–2040 (1990).
18. A. M. Derrington, J. Krauskopf, and P. Lennie, "Chromatic mechanisms in lateral geniculate nucleus of macaque," *J. Physiol.* **357**(1), 241–265 (1984).
19. S. G. Solomon, J. W. Peirce, N. T. Dhruv, and P. Lennie, "Profound contrast adaptation early in the visual pathway," *Neuron* **42**(1), 155–162 (2004).
20. M. A. Webster and J. A. Wilson, "Interactions between chromatic adaptation and contrast adaptation in color appearance," *Vision Res.* **40**(28), 3801–3816 (2000).
21. M. A. Webster and J. D. Mollon, "Colour constancy influenced by contrast adaptation," *Nature* **373**(6516), 694–698 (1995).
22. M. A. Webster and J. D. Mollon, "Adaptation and the color statistics of natural images," *Vision Res.* **37**(23), 3283–3298 (1997).
23. L. E. Welbourne, A. B. Morland, and A. R. Wade, "Human colour perception changes between seasons," *Curr. Biol.* **25**(15), R646–647 (2015).
24. M. A. Webster, Y. Mizokami, and S. M. Webster, "Seasonal variations in the color statistics of natural images," *Network: Comput. in Neural Systems* **18**(3), 213–233 (2007).
25. Y. Mizokami, C. Kamesaki, N. Ito, S. Sakaibara, and H. Yaguchi, "Effect of spatial structure on colorfulness adaptation for natural images," *J. Opt. Soc. Am. A* **29**(2), A118–127 (2012).
26. Y. Mizokami and H. Yaguchi, "Perception of colorfulness influenced by chromatic variance in indoor environments," *J. Light & Vis. Env.* **34**(2), 69–75 (2010).
27. M. D. Fairchild, *Color appearance models* (John Wiley & Sons, 2013).
28. J. Cohen, "Dependency of the spectral reflectance curves of the Munsell color chips," *Psychonomic Sci.* **1**(1-12), 369–370 (1964).
29. L. T. Maloney, "Evaluation of linear models of surface spectral reflectance with small numbers of parameters," *J. Opt. Soc. Am. A* **3**(10), 1673–1683 (1986).
30. D. I. MacLeod and R. M. Boynton, "Chromaticity diagram showing cone excitation by stimuli of equal luminance," *J. Opt. Soc. Am.* **69**(8), 1183–1186 (1979).
31. M. A. Webster and J. D. Mollon, "The influence of contrast adaptation on color appearance," *Vision Res.* **34**(15), 1993–2020 (1994).
32. E. H. Land, "The retinex," *Am. Sci.* **52**, 247–264 (1964).

33. J. Krauskopf, D. R. Williams, and D. W. Heeley, "Cardinal directions of color space," *Vision Res.* **22**(9), 1123–1131 (1982).
34. Z. J. Isherwood, D. S. Joyce, M. K. Parthasarathy, and M. A. Webster, "Pasticity in perception: Insights from color deficiencies," *Faculty Rev.* **9**, 8 (2020).
35. B. C. Regan and J. D. Mollon, "The relative salience of the cardinal axes of colour space in normal and anomalous trichromats," in *Colour Vision Deficiencies* C. R. Cavonius, ed. (Dordrecht, 1997), pp. 261–270.
36. A. E. Boehm, D. I. MacLeod, and J. M. Bosten, "Compensation for red-green contrast loss in anomalous trichromats," *J. Vis.* **14**(13), 19 (2014).
37. K. Knoblauch, B. Marsh-Armstrong, and J. S. Werner, "Suprathreshold contrast response in normal and anomalous trichromats," *J. Opt. Soc. Am. A* **37**(4), A133–A144 (2020).
38. K. J. Emery, M. Kuppuswamy Parthasarathy, D. S. Joyce, and M. A. Webster, "Color perception and compensation in color deficiencies assessed with hue scaling," *Vision Res.* **183**, 1–15 (2021).
39. D. T. Lindsey, A. M. Brown, and L. N. Hutchinson, "Appearance of special colors in deuteranomalous trichromacy," *Vision Res.* **185**, 77–87 (2021).
40. A. E. Boehm, J. Bosten, and D. I. A. MacLeod, "Color discrimination in anomalous trichromacy: Experiment and theory," *Vision Res.* **188**, 85–95 (2021).
41. K. E. M. Tregillus, Z. J. Isherwood, J. E. Vanston, S. A. Engel, D. I. A. MacLeod, I. Kuriki, and M. A. Webster, "Color compensation in anomalous trichromats assessed with fMRI," *Curr. Biol.* **31**(5), 936–942.e4 (2021).
42. J. Rabin, A. Kryder, and D. Lam, "Binocular facilitation of cone-specific visual evoked potentials in colour deficiency," *Clin. & Exp. Optometry: J. Australian Optometrical Assoc.* **101**(1), 69–72 (2018).
43. M. W. Greenlee, M. A. Georgeson, S. Magnussen, and J. P. Harris, "The time course of adaptation to spatial contrast," *Vision Res.* **31**(2), 223–236 (1991).
44. S. Magnussen and M. W. Greenlee, "Marathon adaptation to spatial contrast: saturation in sight," *Vision Res.* **25**(10), 1409–1411 (1985).
45. K. E. Tregillus and S. A. Engel, "Long-term adaptation to color," *Curr. Opinion in Behavioral Sci.* **30**, 116–121 (2019).
46. M. Bao and S. A. Engel, "Distinct mechanism for long-term contrast adaptation," *Proc. Natl. Acad. Sci. U. S. A.* **109**(15), 5898–5903 (2012).
47. O. Yehezkel, D. Sagi, A. Sterkin, M. Belkin, and U. Polat, "Learning to adapt: Dynamics of readaptation to geometrical distortions," *Vision Res.* **50**(16), 1550–1558 (2010).
48. Y. Li, K. E. Tregillus, Q. Luo, and S. A. Engel, "Visual mode switching learned through repeated adaptation to color," *eLife* **9**, e61179 (2020).
49. J. J. Atick, Z. Li, and A. N. Redlich, "What does post-adaptation color appearance reveal about cortical color representation?" *Vision Res.* **33**(1), 123–129 (1993).